STABILITY AND RELAXATION BEHAVIOUR OF SHOT PEENING INDUCED RESIDUAL STRESSES IN AISI 4140 DURING BENDING FATIGUE

H. Holzapfel, V. Schulze, O. Vöhringer, E. Macherauch
Institut für Werkstoffkunde I, Universität Karlsruhe,
Kaiserstr. 12, D 76128 Karlsruhe, FRG

ABSTRACT

Shot peening induced residual stresses can be relaxed by supplying sufficiently high amounts of thermal and/or mechanical energy, which converts the residual elastic strains to microplastic strains. In order to better understand this relaxation behaviour, the steel AISI 4140 (German grade 42 CrMo 4) in a normalized condition and a quenched and tempered condition was investigated in bending fatigue experiments at 25°C, 250°C and 400°C. Characterization of the residual stress changes in shot peened flat specimens during fatigue was realized by X-ray stress measurements. In all cases the residual stress relaxation occurs in different regimes. First, thermal relaxation reduces the residual stresses during specimen heating. Next, relaxation during the first cycle can be discussed on the basis of the effects due to quasistatic loading. Due to cyclic creep effects the interval between the first cycle (N=1) and the number of cycles to crack initiation N_i is characterized by linearly decreasing residual stresses with the logarithm of N. Finally for $N > N_i$ the reduction of residual stresses with logarithm of N is stronger than linearly. In both heat treatment conditions the residual stress relaxation at the three temperatures is similiar and is not accelerated by simultaneous higher temperature and cyclic loading effects. The similiar relaxation behaviour for the different steel conditions investigated is influenced by the separate effects of thermal and cyclic residual stress relaxation. The last one is essentially influenced by dynamic strain ageing processes.

KEYWORDS

bending fatigue, cyclic loading, residual stress relaxation, shot peening treatment

INTRODUCTION

Shot peening is a wide spread technical process whose primary aim is to increase the fatigue limit of components with medium and high hardnesses. The positive effects of shot peening are the introduction of compressive residual stresses in material regions close to the surface and the work hardening of the surface layer [1-8]. Many shot peened components are operated at increased temperatures with cyclic loadings. Since the relaxation of residual stresses may decrease or even eliminate the positive effect of shot peening treatments, the stability of residual stresses at cyclic loadings and increased temperatures is very important. Therefore this report deals with investigations on residual stress relaxation during bending fatigue at room temperature and increased temperatures of shot peened AISI 4140 (German grade 42 CrMo 4) in a normalized condition and a quenched and tempered condition.

MATERIAL, HEAT TREATMENTS AND EXPERIMENTAL PROCEDURE

The steel AISI 4140 (German grade 42 CrMo 4), which is often used in practical applications in a quenched and tempered condition, was used in the current experiments. The chemical composition was 0.44 C, 1.05 Cr, 0.21 Mo, 0.22 Si, 0.59 Mn, 0.06 Ni, 0.02 P, 0.01 S and the rest Fe (all in weight-%). Flat specimens with a cross section of 2 x 18 mm^2 were heat treated in a vacuum quenching furnace. The specimens of the normalized condition were austenitized at 930°C for 3h and slowly cooled down in the furnace. The quenched and tempered condition (T450) was produced by austenitizing for 20min at 850°C, oil quenching down to 25°C, tempering at 450°C for 2h and finally slow cooling in the furnace. The shot peening treatments were performed on an in-house air blast machine. By simultaneous peening of both surfaces shot peening induced distortions are avoided. Cast steel shot S170 (medium diameter 0.43 mm, 46 HRC) was used at a pressure of 1.6 bar and a flow rate of 1.5 kg/min, which resulted in a 98% coverage. The bending fatigue experiments were performed on alternating bending machines at 25 Hz with heating elements at the grips. This allowed for test temperatures of 250°C and 400°C. Before and after each experiment, the residual stresses were measured using the X-ray technique. Residual stresses were determined using the $\sin^2\psi$-method [9] with CrKα-radiation on the {211}-plane of the bcc phase and at ψ-angles in the range $-45° \leq \psi \leq +45°$. For the experiments with T > 25°C each measurement required a new specimen. Room temperature measurements for one fictitious initial stress amplitude at the surface were all performed with a single specimen by interrupting the test at selected numbers of cycles, making X-ray measurements and then restarting the test. The residual stresses of the shot peened specimens were measured either on the upper side of the specimens (the side first loaded in compressive direction) or on the lower side. The measurement position will be indicated in either the text or the figures. The residual stresses were measured in the direction in which the bending stresses acted (longitudinal), as well as in the transverse direction. The measurement of the depth distribution of the residual stresses was performed by iterative electrolytical removal of thin surface layers and subsequent X-ray measurements. Correction for the surface removal was performed [10].

EXPERIMENTAL RESULTS

Characterization of the shot peened surface layer

In the normalized condition, the magnitudes of residual stresses decrease continuously from 380 N/mm^2 at the surface to zero at a distance from the surface equal to 0.3 mm. In the quenched and tempered condition, constant residual stresses of -600 N/mm^2 are measured up to a depth of 0.15 mm. At greater distances from surface, the residual stresses rapidly decrease to zero at 0.225 mm. While the half width breadths of the diffracted peaks in the surface region of the normalized specimens increased from 2.0°2θ to 2.7°2θ as a result of shot peening, no significant change of the half width breadths of about 3.2°2θ was observed for the quenched and tempered specimens.

Normalized condition

Fig. 1a) shows examplarily the magnitudes of residual stresses in the longitudinal and transverse directions at a fictitious initial stress amplitude at the surface of $\sigma^*_{a,S}$ = 400 N/mm^2. After half of the first loading cycle, the residual stresses on the upper side of

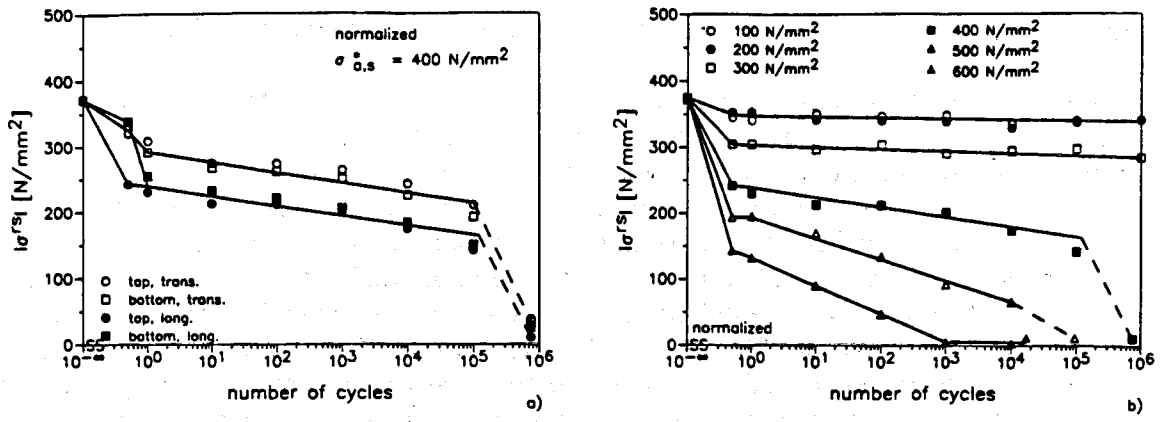

Fig. 1: Magnitudes of residual stresses σ^{rs} vs. number of cycles for the normalized condition, (a) at a fictitious initial stress amplitude at the surface of $\sigma^*_{a,S}$ = 400 N/mm² (upper and lower side, longitudinal and transverse), (b) at various $\sigma^*_{a,S}$-values (upper side, longitudinal).

the specimen are reduced from -375 N/mm² to -245 N/mm² by the compressive loading. The lower side, which was loaded in tension, shows a minor relaxation of residual stresses. After the first full cycle, the residual stresses on the upper and lower sides are similar to each other because of a strong relaxation on the lower side. Forup to 10^5 cycles, the further relaxation of residual stresses occurs almost linearly with the logarithm of the number of cycles. Between 10^5 cycles and failure at 747400 cycles, the reduction in residual stresses occurs more rapidly than before. The changes in residual stresses in the transverse direction are always slower than in the longitudinal direction.

Fig. 1b) presents the trends of the magnitudes of the residual stresses at the upper side vs. the number of cycles for different fictitious initial stress amplitudes at the surface. The value at N = $10^{-\infty}$ corresponds to the mean value of all initial residual stresses measured. With increasing load amplitude the residual stresses relax more rapidly. A linear correlation between residual stresses and the logarithm of the number of cycles can again be recognized over wide intervals of number of cycles. The residual stress distributions in the longitudinal direction remaining after either failure or 10^6

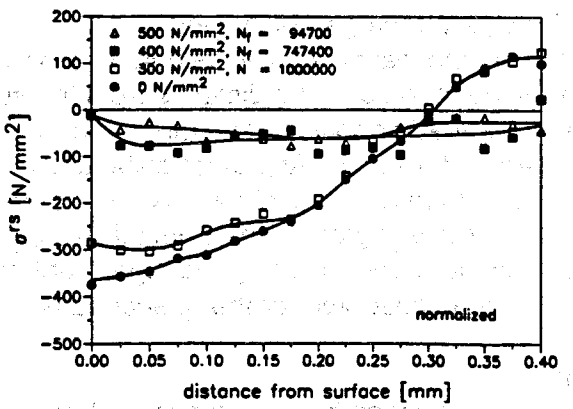

Fig. 2: Residual stresses vs. distance from the surface at different $\sigma^*_{a,S}$-values for the normalized condition (upper side, longitudinal).

cycles were measured for specimens loaded with $\sigma^*_{a,S}$ = 300, 400 and 500 N/mm^2 and are plotted in Fig. 2 together with the depth distribution of residual stresses directly after shot peening. It is seen, that the strongest relaxation of residual stresses occurs in the area close to the surface.

Fig. 3 examplarily shows the changes in residual stresses in the longitudinal direction at the upper side vs. number of cycles at $\sigma^*_{a,S}$ = 300 N/mm^2 for 25, 250 and 400°C. In this figure, the values at N = $10^{-\infty}$ correspond to the values which were measured after heating up to the testing temperature and waiting for temperature compensation between specimen surface and core. The residual stresses are reduced to -350 N/mm^2 by heating to 250°C and to -300 N/mm^2 by heating to 400°C. The $|\sigma^{rs}|$,N-trends are very close to each other and do not differ by more than 50 N/mm^2.

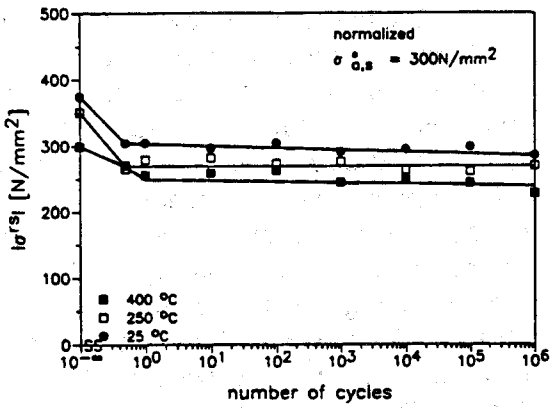

Fig. 3: Magnitudes of residual stresses vs. number of cycles at $\sigma^*_{a,S}$ = 300 N/mm^2 and at various temperatures for the normalized condition (upper side, longitudinal).

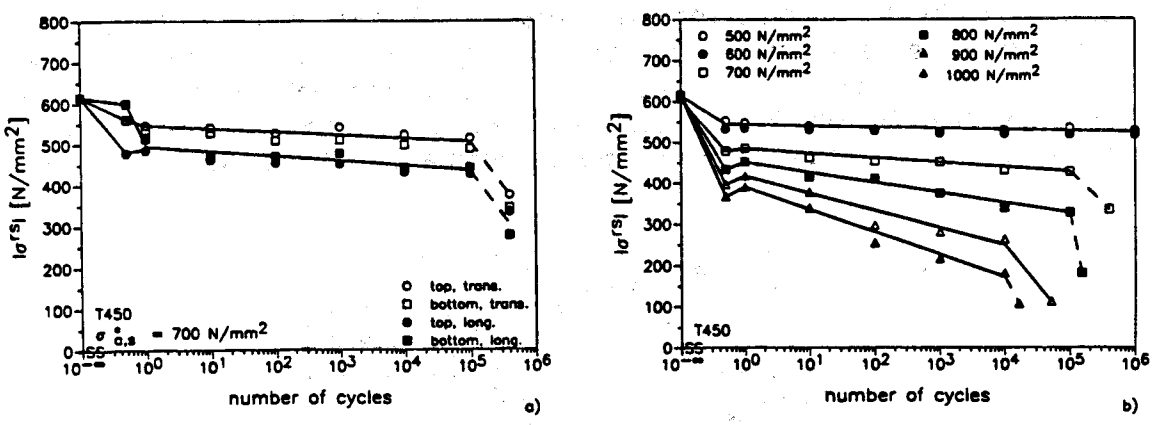

Fig. 4: Magnitudes of residual stresses σ^{rs} vs. number of cycles for the quenched and tempered condition, (a) at a fictitious initial stress amplitude at the surface of $\sigma^*_{a,S}$ = 700 N/mm^2 (upper and lower side, longitudinal and transverse), (b) at various $\sigma^*_{a,S}$-values (upper side, longitudinal).

Quenched and tempered condition

Fig. 4a) shows the trends of the magnitudes of residual stresses vs. number of cycles in the longitudinal and transverse directions at a fictitious initial stress amplitude at the surface of 700 N/mm^2. The upper side, loaded in compressive direction in the first half

cycle, shows relaxation of the residual stresses from -600 N/mm^2 to about -480 N/mm^2. During this first half cycle, the lower side shows no considerable relaxation. In the second half cycle, this trend is reversed and the residual stresses measured at the upper and the lower side are similar. In the course of further cyclic loading up to 10^5 cycles the residual stresses reduce linearly with the logarithm of the number of cycles. After failure of the specimen at N=399900 further reductions in the magnitudes of the residual stresses are measured. The residual stresses in the transverse direction always relax more slowly than in the longitudinal direction.

For fictitious initial stress amplitudes at the surface between 500 and 1000 N/mm^2 Fig. 4b) summarizes the changes in residual stresses measured at the upper side of the specimens as a function of the logarithm of the number of cycles. As for the normalized condition, the value at N = 10^{∞} corresponds to the mean magnitude of all initial residual stresses measured. In the first half cycle, relaxation of the residual stresses which increases with increasing loading amplitude is observed. The second half cycle, for which the upper side is loaded in tension, leads to a small increase in the magnitudes of surface residual stresses. Further relaxation of residual stresses at all amplitudes investigated can be approximated over a wide range of the logarithm of number of cycles by a straight line. The slope of this line increases with increasing fictitious initial stress amplitude at the surface. At failure, once more, further reduction of the residual stresses occurs. For the specimens loaded with $\sigma^*_{a,S}$ = 600, 700 and 800 N/mm^2 the depth distributions of the remaining residual stresses were determined after either failure or 10^6 cycles. This is shown in Fig. 5 together with the residual stress distribution directly after shot peening ($\sigma^*_{a,S}$ = 0 N/mm^2). The residual stresses reduce primarily in the area close to the surface and the relaxation is stronger for higher fictitious initial stress amplitudes at the surface. Increasing relaxation of residual stresses leads to a tendency for an increase in depth at which zero residual stresses are measured.

Fig. 6 shows the relaxation of residual stresses at 25, 250 and 400°C for $\sigma^*_{a,S}$ = 600 N/mm^2. Here the values at N = 10^{∞} for 250 and 400°C correspond to the residual stresses measured after specimen heating. The values are -550 N/mm^2 at 250°C and -375 N/mm^2 at 400°C. I the first half cycle, the magnitudes of the compressive residual stresses at the upper side of the specimens loaded at 250°C and 400°C show similar

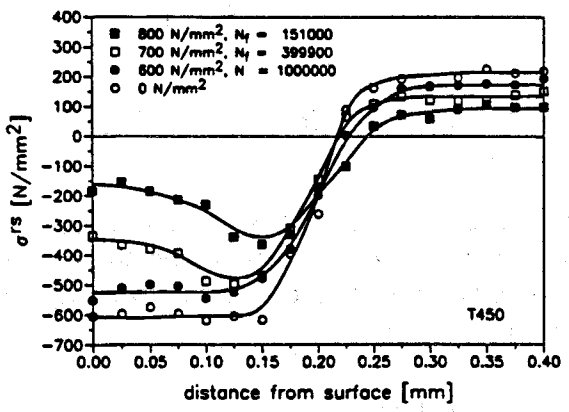

Fig. 5: Residual stresses vs. distance from the surface at different $\sigma^*_{a,S}$-values for the quenched and tempered condition (upper side, longitudinal).

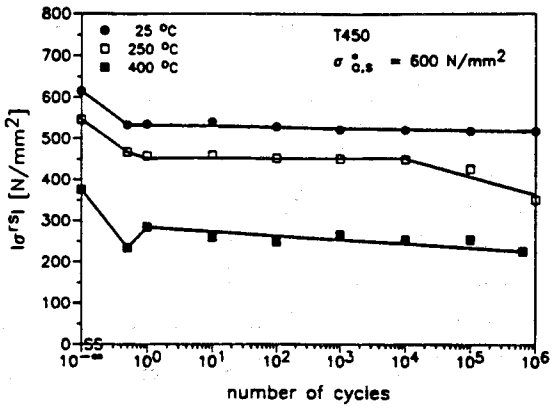

Fig. 6: Magnitudes of residual stresses vs. number of cycles at $\sigma^*_{a,S}$ = 600 N/mm² and at various temperatures for the quenched and tempered condition (upper side, longitudinal).

relaxation as at 25°C. In the second half cycle, however, an increase of the compressive residual stresses is observed at 400°C. In the further course of the cyclic loading somewhat larger rates of relaxation than at 25°C are observed at 250°C for $N>10^4$ and at 400°C for $N>1$.

DISCUSSION

First of all the results at 25°C should be considered and evaluated. The apparent residual stress relaxation can be subdivided into three phases because of different characteristic phenomena. The relaxation behaviour for $N \leq 1$ is caused by quasistatic deformation processes and for $1 \leq N \leq N_I$ (N_I = number of cycles to crack initiation) by cyclic deformation processes. They lead to a linear reduction in residual stresses as a function of the logarithm of the number of cycles. For $N_I < N \leq N_f$ (N_f = number of cycles to failure) the relaxation rate for sufficiently high fictitious initial stress amplitudes at the surface is increased by initiation of surface cracks and crack propagation as well as by failure of the specimen.
The sequence of residual stress relaxation in the first cycle is determined by the inhomogeneous stress distribution over the cross-section of the specimens resulting from the bending loading. Thus the upper side of the specimen is loaded compressively in the first half loading cycle. These compressive stresses superpose themselves with the compressive residual stresses in the region close to the surface. If the resulting stresses are larger than the surface compressive yield stress $R_{e(c),S}$, plastification starts and this results in relaxation of the residual stresses. As a result of stress equilibrium, a small relaxation at the lower side can also appear. Furthermore, the resultant stress on the lower side in the first half cycle is reduced slightly as a result of the compressive residual stresses being superposed with tensile loading stresses. Fig. 7 represents the dependence of residual stresses at the upper side (compressive loading) and lower side (tensile loading) on the fictitious stress at the surface σ^*_S after the first half cycle for both heat treatments investigated. For the normalized condition residual stress relaxation is observed at fictitious compressive stresses at the surface which are higher than 200 N/mm². For further increase of load amplitudes the normali-

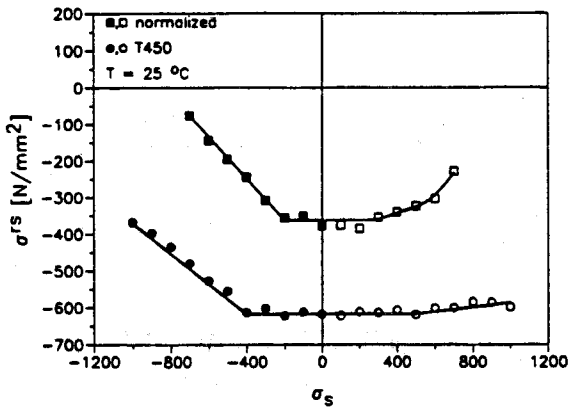

Fig. 7: Residual stresses vs. fictitious initial stress amplitude at the surface after the first half cycle (normalized condition and quenched and tempered condition, upper side, longitudinal).

zed specimens show a constant rate of relaxation. On the side loaded in tension a slight residual stress relaxation which starts at higher loads is recorded. For the quenched and tempered condition the relaxation at the upper side (loaded in compression) starts at $\sigma_S^* = -400$ N/mm^2 and displays at a constant rate of relaxation for increased bending amplitudes. The lower side (loaded in tension) shows a minor decrease of the residual stresses for loading stresses $\sigma_S^* \geq 500$ N/mm^2. This is believed to be caused by stress equilibration after the strong residual stress relaxation which occurs simultaneously at the upper side. A procedure described in [11] allows the determination of the surface compressive yield stresses $R_{e(c),S}$. This leads to $R_{e(c),S} = -486$ N/mm^2 for the normalized condition ($R_{e(c),unpeened} = -345$ N/mm^2) and $R_{e(c),S} = -890$ N/mm^2 for the quenched and tempered condition ($R_{e(c),unpeened} = -1300$ N/mm^2). Comparison with the compressive yield stress of the unpeened conditions listed in the parenthesis leads to the conclusion, that shot peening results in a surface workhardening of the normalized condition and in a surface worksoftening of the quenched and tempered condition. These findings qualitatively agree with results of residual stress relaxation experiments due to quasistatic loading of the same steel condition [12].
In the second half cycle the situation is reversed. The upper side now undergoes tensile loading, whereas the lower side undergoes compressive loading. Consequently residual stress relaxation now predominantly occurs on the lower side of the specimens. While for the normalized condition the residual stresses at the upper side remain nearly constant, they slightly decrease their magnitudes for the quenched and tempered condition. The decrease is more significant for higher initial stress amplitudes at the surface (see. Fig. 4b). This results from the residual stresses set up from bending, which show negative values at the tensile side after lowering the bending load. This is possible, because the compressive deformation of the upper side in the first half cycle can be regarded as a predeformation for the tensile loading in the second half cycle. Thus a distinctive Bauschinger-effect results for quenched and tempered specimens [13], which reduces the tensile yield stress such that relatively slight resulting tensile stresses at the upper side in the second half cycle are sufficient to cause plastification. These results are summarized in Fig. 8 which presents the ratio of the residual stresses after the first half loading cycle to its initial value vs. the initial load amplitude at surface, $\sigma_{a,S}^*$. The remaining residual stresses for both heat treat-

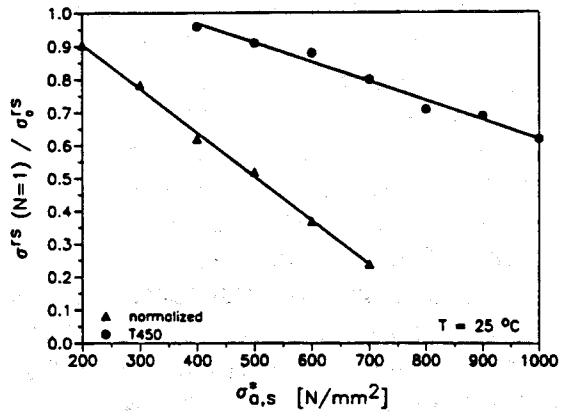

Fig. 8: Ratio $\sigma^{rs}(N=1)/\sigma^{rs}$ vs. fictitious initial stress amplitude at the surface (normalized condition and quenched and tempered condition, upper side, longitudinal).

ments show trends which depend linearly on $\sigma^*_{a,S}$. For the normalized condition the relaxation is larger than for the quenched and tempered condition because of the lower strength.
At larger numbers of cycles the residual stresses reduce linearly with the logarithm of the number of cycles according to the following relation:

$$\sigma^{rs} = A + m \lg N \qquad (1)$$

As can be seen from Fig. 9, the magnitude of the slope m of this straight line is linearly influenced by the fictitious initial stress amplitude at the surface. This can be described by straight lines with similar slopes for both heat treatments. The residual stress relaxation occuring at $1 < N < N_l$ can be traced back to cyclic plastic deformations. They occur if the cyclic yield stress is reached for the given stress amplitude. Thus the arrangements of dislocations which exist after shot peening are changed to configurations, which are typical for fatigue loading [14]. So, for instance, cell structures develop for the normalized condition with increasing fatigue loading amplitudes and numbers of cycles [15].

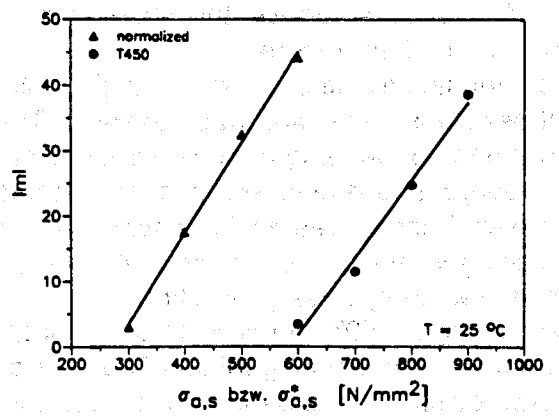

Fig. 9: Magnitude of the slope $m = d|\sigma^{rs}|/d \lg N$ vs. fictitious initial stress amplitude at the surface (normalized condition and quenched and tempered condition, upper side, longitudinal).

After failure the final relaxed state of the residual stresses cannot be estimated from the linear relation which was valid before. Considering the change of the number of microcracks which appear on the surface [16], it is believed that the increased reduction in residual stresses is caused by local plastifications at the tips of cracks.
At higher temperatures the relaxation of residual stresses is stronger because of the additional contribution of thermal residual stress relaxation during specimen heating. The residual stresses are thus reduced to levels, which are characteristic for the corresponding temperatures. The residual stress relaxation in the first loading cycle can be explained by the already discussed mechanisms for residual stress relaxation under quasistatic loading at room temperature. Because of the inhomogeneous stress distribution over the cross-section of the specimen during bending loadings, the deformation behaviour of the surface layer is of primary interest.
In the temperature range between 25°C and 400°C, for the normalized condition dynamic strain ageing occurs [17]. This causes similar stress-strain curves at the surface for 25°C, 250°C and 400°C [11]. If at the upper side of the specimen (loaded in compression) during the first half cycle the sum of the loading and residual stresses or the equivalent stress reach the surface compressive yield stress, then residual stress relaxation occurs. Because of the similar stress-strain curves for the different temperatures at the normalized condition the residual stress relaxation at N = 0.5 will be almost equal. The differences in measured values may be caused by minor uncertanties in the measurements (see Fig. 3). During subsequent cyclic loadings the magnitudes of residual stresses are reduced only slightly. This is a surprising result, because at least at 400°C after $N=10^6$ (=11.1h elapsed time) a larger residual stress relaxation was expected as a result of cyclic and thermal loading and additional cyclic creep effects. Evidently dynamic strain ageing hinders the larger cyclic microplastifications which are necessary for residual stress relaxation.
In contrast to the normalized condition for the quenched and tempered condition a clear dependence of the residual stress relaxation on temperature can be seen within the first cycle. After the first half cycle, the corresponding residual stress magnitudes at 25 °C are clearly higher than the magnitudes measured after loading at 250°C and 400°C. This finding is qualitatively in agreement with results of quasistatic tests [11,12]. A distinct dependence of the stress-strain curves on temperature exists at this heat treatment condition [11]. As discussed above, this should cause a strong dependence of residual stress relaxation on temperature.
During the transition from the first to the second half cycle at 400°C an increase in the compressive residual stress at the upper side was observed. This phenomenon can be traced back to the occurrence of bending residual stresses at elastic-plastic loading, since the upper side undergoes tensile stresses in the second half cycle and consequently shows compressive bending residual stresses after unloading. Like at room temperature, the Bauschinger-effect leads to yield at very low tensile stresses and therefore causes a further residual stress generation.
During the further cyclic loading at 250°C for $N > 10^4$ and at 400°C for $N > 1$ somewhat larger rates of relaxation with increasing logarithm of number of cycles are measured. This is essentially caused by time-dependent thermal relaxation of residual stresses. It visibly progresses at 250°C after 10^5 and 10^6 cycles (corresponding to experimental times of 1.1h and 11.1h) and at 400°C already after relatively short annealing times [18].

SUMMARY

The relaxation of residual stresses caused by bending fatigue loading at 25°C can be divided into several phases. During half of the first loading cycle the residual stresses are reduced on the compressively loaded side more than on the one loaded in tension. In the second half cycle the situation is reversed. For numbers of cycles $1 < N < N_1$ the residual stresses reduce linearly with increasing logarithm of the number of cycles. The slope of this straight line is linearly dependent on the fictitious initial stress amplitude at the surface. For $N > N_1$ the residual stresses reduce more rapidly. The residual stresses in the transverse direction always decrease more slowly than in the longitudinal direction.
The residual stress relaxation caused by bending fatigue loading of normalized specimens at 250°C and 400°C is marked by measurements, which are quite close to the values at room temperature. This presumably results from dynamic strain ageing processes. For quenched and tempered specimens the measured values of residual stresses at different temperatures are clearly separable because of different effects during the first loading cycle. For $N > 1$ the rates of residual stress relaxation at all 3 test temperatures are similar. Only for long experimental times the still occurring thermal relaxations of residual stresses at 250°C and 400°C cause slightly larger relaxation rates.

ACKNOWLEDGEMENT

The financial support for these investigations by the Deutsche Forschungsgemeinschaft is gratefully acknowledged.

LITERATURE

[1] A. Niku-Lari (ed.): Proc. Int. Conf. Shot Peening 1, Paris, 1981, Pergamon Press Oxford, 1982.
[2] H. O. Fuchs (ed.): Proc. Int. Conf. Shot Peening 2, Chicago, 1984, The American Shot Peening Society, Paramus New York, 1984.
[3] H. Wohlfahrt, R. Kopp, O. Vöhringer (eds.): Proc. Int. Conf. Shot Peening 3, Garmisch-Partenkirchen, 1987, DGM Informationsgesellschaft, Oberursel, 1987.
[4] K. Iida (ed.): Proc. Int. Conf. Shot Peening 4, Tokyo, 1990, The Japan Society of Precision Engineering, Tokyo, 1990.
[5] D. Kirk (ed.): Proc. Int. Conf. Shot Peening 5, Oxford, 1993, Coventry University, Oxford, 1993.
[6] B. Scholtes: Eigenspannungen in mechanisch randschichtverformten Werkstoffzuständen-Ursachen, Ermittlung und Bewertung, DGM Informationsgesellschaft, Oberursel, 1991.
[7] E. Macherauch, H. Wohlfahrt, R. Schreiber et al.: Verbesserung der Bauteileigenschaften durch Strahlen, HFF-Bericht Nr.6, Umformtechn. Kolloquium Hannover, 12/13.3.1980.
[8] F. Burgahn, O. Vöhringer, E. Macherauch: Microstructural investigation of the shot peened steel 42CrMo4 in different heat treatment conditions by the aid of a X-Ray profile analysis, in [4], 199-207.

[9] E. Macherauch, P. Müller: Das $\sin^2\Psi$-Verfahren der röntgenographischen Spannungsmessung, Z. f. angew. Physik 7 (1961), 305-312.
[10] M.G. Moore, W.P. Evans: Mathematical correction for stress in removed layers in X-Ray diffraction residual stress analysis, Trans. SAE 66 (1958), 340-345.
[11] H. Holzapfel: Das Abbauverhalten kugelstrahlbedingter Eigenspannungen bei 42CrMo4 in verschiedenen Wärmebehandlungszuständen, Dr.-Ing. Dissertation, Universität Karlsruhe (TH), 1994.
[12] H. Holzapfel, V. Schulze, O. Vöhringer, E. Macherauch: Relaxation Behaviour of Shot Peening Induced Residual Stresses in AISI 4140 due to Quasistatic Loading at Elevated Temperatures, these proceedings.
[13] H. Hanagarth, O. Vöhringer, E. Macherauch: Relaxation of Shot Peening Residual Stresses of the Steel 42CrMo4 by Tensile or Compressive Deformation, In: [4], 337-345.
[14] O. Vöhringer: Abbau von Eigenspannungen, in E. Macherauch, V. Hauk (eds.) "Eigenspannungen, Entstehung-Messung-Bewertung", DGM Informationsgesellschaft, Oberursel (1983), Bd.1, 49-83.
[15] D. Eifler: Inhomogene Deformationserscheinungen bei Schwingbeanspruchung eines unterschiedlich wärmebehandelten Stahles des Typs 42CrMo4, Dr.-Ing. Dissertation, Universität Karlsruhe (TH), 1981.
[16] A. Ebenau: Das Verhalten von kugelgestrahltem 42CrMo4 im normalisierten und vergüteten Zustand unter einachsig homogener und inhomogener Wechselbeanspruchung, Dr.-Ing. Dissertation, Universität Karlsruhe (TH), 1989.
[17] K. Hüttebräucker, O. Vöhringer, E. Macherauch: The Influence of Alloying to the Onset of Dynamic Strain Ageing of Steels with Low Carbon Content, In: P. Haasen, G. Kostorz (eds.), Proc. ICSMA 5, Aachen, Pergamon Press New York, Vol. 2, 1037-1042.
[18] V. Schulze, F. Burgahn, O. Vöhringer, E. Macherauch: Zum thermischen Abbau von Kugelstrahleigenspannungen bei vergütetem 42CrMo4, Mat.-wiss. u. Werkstofftech. 24 (1993), 258-267.